Size, Shape and Functionality Dependence of Solute Transport Mechanisms in a Cross-linked H_{II} Phase Lyotropic Liquid Crystal Membrane

Benjamin J. Coscia   Michael R. Shirts

March 5, 2019

1   Introduction

We need highly selective membranes in order to perform efficient separations.

H_{II} phase lyotropic liquid crystals have densely packed, uniform sized pores and have the potential to disrupt conventional membrane separation techniques by being selective based not only on size and charge, but on chemical functionality as well.

We can only learn so much from experiment. MD can give us mechanistic insights with atomistic resolution so that we can intelligently design new membranes for solute-specific separations.

In previous work, we determined the most likely structure of the hexagonal phase formed by the monomer Na-GA3C11.

- We developed techniques for equilibrating the hexagonal phase made by neat monomer as well as with varying amounts of water in the pores.

In this work, we have studied the transport mechanisms exhibited by a number of polar solutes with varying size, chemical functionality and hydrophilic character.

- Many of the separations we are interested in involve polar organic compounds.

There are a number of questions we wish to address in order to characterize transport in this system.

1. What transport mechanisms do we observe?

   Given that the pores will restrict motion of the solutes, we anticipate that transport will be hindered in some way. We want to understand the differences in solute motion, specifically its mean squared displacement (MSD), based on a solute's size, shape and chemical functionality. We will study the interactions between solutes, the membrane, and water in order to determine which mechanism or mechanisms dominate.

2. How do molecules, including water, partition within the pores?

   From a macroscopic perspective, it is straightforward to hypothesize that the water and polar solutes spend their time exclusively in the tube-like hydrophilic pore region. Our previous work showed that there is a gradual compositional transition from the hydrophilic to the hydrophobic region which means that solutes may not necessarily stay confined to the centers of the pores or even within the pore region. We will study the gradient in composition of solutes and water and any resultant influence it might have on mechanistic properties.

3. Can we describe the transport mechanisms using pre-existing mathematical models.

   A mathematical model may provide additional insight into the transport mechanisms and, in future work, can help relate performance on the timescales studied with MD to macroscopic timescales. We will use qualitative and semi-quantitative arguments in order to choose a governing model.

4. How can we modify the current monomers in order to enhance solute-specific separations?

   Most experimental characterization up to this point has been centered around the monomer, Na-GA3C11, studied here. The primary reason for conducting these simulations is to understand what chemical modifications can be made to this or similar liquid crystal molecules in order to enhance transport of desired species or restrict that of undesired species. We will use the insight gained from our mechanistic observations in order to suggest new monomer designs.

There are also a number of questions this study is not intended to answer.

- We will not study the concentration dependence of the observed transport rates. Although the average MSD might change with concentration, we are focused on the underlying solute-membrane interactions that lead to the observed transport mechanisms which we conjecture will be the same regardless of concentration.

- We will not study the chemical potential of solutes in the pores, which could give us a better understanding of equilibrium solute partitioning. This information will not greatly enhance our understanding of mechanistic details in various membrane regions.

- Both of the above points will add unnecessary levels of complexity which can be left for a future study.

- This work is a simple starting point meant for observing the types of interactions which occur between isolated solutes and the membrane.

2 Methods

System Setup

Stable H_{II} phases, assembled with Na-GA3C11, can be formed using a broad range of water concentrations.

- In the literature, this system is typically synthesized with close to 10 wt % water [1, 2]

- However, Resel et al. noted that the system is likely fully hydrated with less than 7 wt % water. [3]

- We decided to test two different levels of water content: 5 and 10 wt %

We observed that water partitions into the tail region of our system and therefore built our initial configurations with water in both regions close to the expected equilibrium value.

- There is about 2:1 water in the pores versus in the tails for the 10 wt % system.

- The amount of water present in the tails may or may not be experimentally consistent but if we don't put it in, the results will not be thermodynamically consistent, which will give issues with measurements and calculations.

- See supporting info for water equilibration simulation data.

- We adjusted the pore radius in our systems so that the right amount of water fits in the pores without any vacuum using `gmx solvate`.

- We placed water molecules in the tail region one at a time in random locations with short energy minimizations between insertions.

We equilibrated an initial solvated configuration before adding solutes.

- We equilibrated the initial configuration using the 'wet' equilibration procedure described in our previous work [4].

- We cross-linked the equilibrated solvated configuration using the cross-linking procedure described in our previous work.

We added 6 solute molecules to each pore of the equilibrated cross-linked configuration.

- We equally spaced each solute in the pore

- 6 solutes per pore provided a balance of a useful amount of data for generating statistics and a low degree of interaction between solutes (reference to supporting information to show low degree of interaction)

- At each insertion point we placed a randomly oriented solute molecule then ran a short energy minimization.

- We allowed the solutes to equilibrate for 5 ns using berendsen pressure control

- We collected transport data using 1 μs simulations

Mean Squared Displacement

We measured the time-averaged z-direction mean squared displacement (MSD) of the centers of mass of each solute over the course of 1 μs MD simulations using Equation 1.

-
$$\overline{x^2(\tau)} = \frac{1}{T - \tau} \int_0^{T-\tau} (x(t + \tau) - x(t))^2 dt \tag{1}$$

  where τ is the time lag and T is the length of the trajectory [5].

- Generally, the MSD grows according to Equation 2,
$$\langle x^2(t) \rangle = K_\alpha t^\alpha \tag{2}$$

- where α is the anomalous exponent and K_α is the generalized diffusion coefficient.

- A value of $\alpha < 1$ indicates a subdiffusive process, while a value of $\alpha = 1$ and $\alpha > 1$ is characteristic of Brownian and superdiffusive motion respectively.

- In practice, α corresponds to the growth of the *ensemble* MSD given by Equation 3 [5]:
$$\langle x^2(t) \rangle = \langle x(t) - x(0) \rangle \tag{3}$$

- The ensemble MSD is calculated with respect to a reference position and hence carries some dependence on its starting point.

- The time-averaged MSD averages over all possible time lags of a given length, effectively eliminating any initial configuration dependence and generating an increased number of observations.

- For ergodic systems, both types of MSDs will be equal.

- Since we have a small number of solutes with which to generate statistics and because we are not calculating values for α in this particular study, we will only use the time-averaged MSD.

We fixed the length of each simulated trajectory so that we could compare the total MSD between different solutes without the influence of the ageing phenomenon.

- Ageing is defined by the tendency of the average MSD to decrease as the length of trajectories are increased [6].

- The maximum measured dwell time can be no longer than the total length of a simulated trajectory.

- As measurement time or trajectory length is increased, longer dwell times are incorporated into the calculation, lowering the average MSD. (See supporting info for demonstration)

- Because the MSDs are non-linear and because of the ageing phenomenon, we did not attempt to calculate a diffusion constant as one might for a Brownian particle with a linear MSD.

- Instead, the reported values for MSD represent the average MSD for a given solute after a 400 ns time lag.

3

Dwell and Hop Length Distributions

We measured the distribution of dwell times and hop lengths in order to test the hypothesis that solutes follow a CTRW process.

- We used the `ruptures` python package in order to identify breakpoints, times when hops occur, in solute trajectories.[7] (See Supporting Information for more details on chosen parameters. i.e. type of cost function, cost function penalty tolerance, number of dimensions used)

- The corresponding hop lengths and dwell times between break points were used to construct empirical distributions.

Radial Density Functions

We measured the average radial distance of each solute of interest from the pore centers.

- We binned the radial distances and then normalized by the volume of the annulus defined by the bin edges.

- Although the pores are often described as straight, they have a small degree of tortuosity which disrupts the RDF calcuation

- We obtain the best RDF by constructing splines that run through the pore centers.

- We construct the splines by dividing the membrane into 10 slices in the z-direction. Within each slice, we calculate the location of the pore centers based on the average location of the aromatic rings that make up the monomer head groups.

- When calculating the RDF, the radial distance from the pore center is based on the distance between the solute center-of-mass and the linearly interpolated (x, y) coordinates of the pore center calculated based on the spline.

Identification of Hydrogen Bonds

Based on the geometric criteria proposed by Luzar and Chandler [8], we determined a hydrogen bond to exist if the distance between the donor, D, and acceptor, A, atoms is less than 3.5 Å and the angle formed by D–H...A is less than 30°.

- Attempts to describe a hydrogen bond in the context of molecular simulations has yielded a number of definitions with no true consensus [9].

- The geometry of hydrogen bonds has some dependence on the system being studied.

- The definition of Luzar and Chandler is easily visualized for trajectories using the `hbonds` representation of the Visual Molecular Dynamics (VMD) software package which allows us to directly check the validity of identified hydrogen bonds.

Coordination number

We quantified the coordination of solutes with surrounding molecules.

- For each frame, we counted the identities and number of coordinated molecules to a given solute based on a distance cut-off.

- We found that this approach is more useful than calculating the 3D spherical radial distribution function because it gives detailed frame-by-frame information rather than an average.

Using four different methods, Rowley and Roux observed peaks in the radial distribution function for sodium coordinated with water at an O-Na distance of between 2.3 and 2.5 Å [10]. We used 2.5 Åas the distance cutoff.

3 Results and Discussion

Structure and Transport of Membrane Constituents

In contrast to our previous work with a solvent-free version of this membrane, the pore region of the 5 and 10 wt % water systems are primarily filled with water and sodium ions.

- In dry systems, the pore center is densely filled with sodium ions and head groups (See Ref [4]).

- Figure 1 plots the densities of each membrane constituent.

- Water is densest at the center of each pore.

- Sodium ions are densest between the pore center and the peak head group density.

- The peak density of sodium ions is not at the pore center in either case likely because they are still loosely associated with the monomer's carboxylate head groups.

Pores in the 10 wt% water system are wider and less crowded by monomers than those in the 5 wt% water system.

- The peak head group density of 10 wt% water systems is about 0.2 nm further from the pore center than the 5 wt%

- The 5 wt % water system has a non-negligible amount of tail group atoms that occupy the pore center.
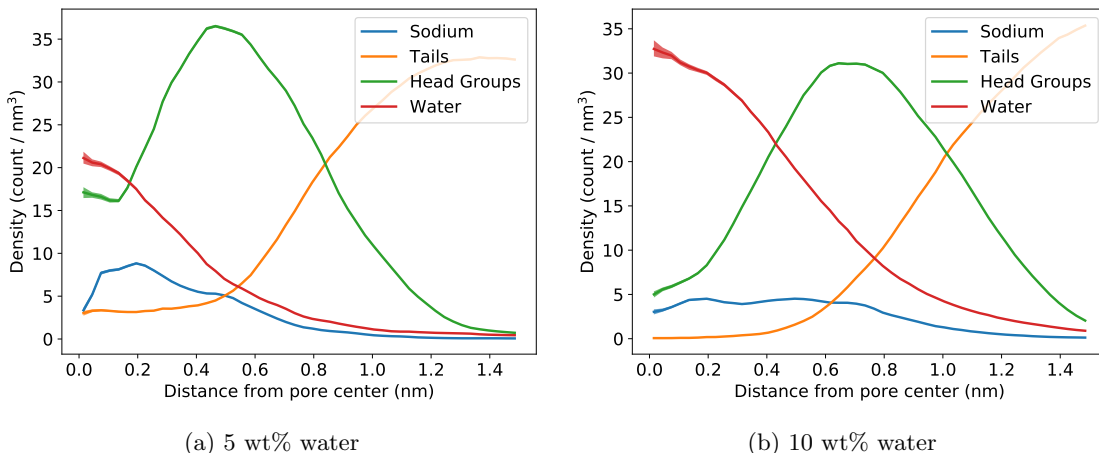

(a) 5 wt% water   (b) 10 wt% water

Figure 1: The radial densities of various monomer components paint a picture of the pore topology where the pore centers are primarily composed of water and sodium ions. The 5 wt % system (a) appears to be much more crowded by monomers than the 10 wt % system (b). Head groups in (a) are densest closer to the pore center than in (b). A small amount of tail components find their way close to the pore center of the 5 wt % system.

Water's mobility is increased when pores are larger and less crowded.

- The MSD of water is about 65 times higher and the MSD of sodium is about 40 times higher in the 10 wt% system.

- Water moves about 65 times faster than sodium in the 10 wt % system and 40 times faster than sodium in the 5 wt % system.

- The diffusivity of water in the 10 wt % system is still only 1 % that of bulk water

Sodium coordinates with far less water molecules than it does in bulk solution.
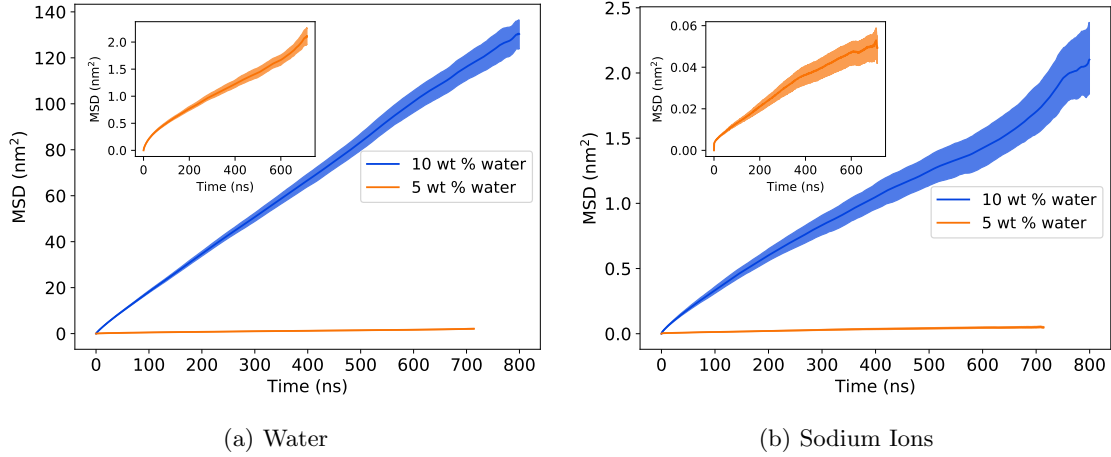
(a) Water

(b) Sodium Ions

Figure 2: (a) The MSD of water in the 10 wt % water system is about 65 times higher than water in the 5 wt % water system. (b) The MSD of sodium in the 10 wt % water system is about 40 times higher than sodium in the 5 wt % water system.

- In bulk water, it is estimated that sodium coordinates with 5.6 - 5.8 water molecules [10]

- In our system, on average, each sodium ion is coordinated to about 1.7 water molecules in the 10 wt % system and 1.15 water molecules in the 5 wt% system.

- The low levels of water coordination under confinement are likely driven in part by favorable interactions between sodium ions and carboxylate head groups.

- A dehydrated sodium ion is not shielded from the negatively charged carboxylate group. [11]

- On average, sodium ions coordinate with 0.5 head group oxygen atoms in the 10 wt % water system and 0.4 head group oxygen atoms in the 5 wt % water system.

(a)

(b)
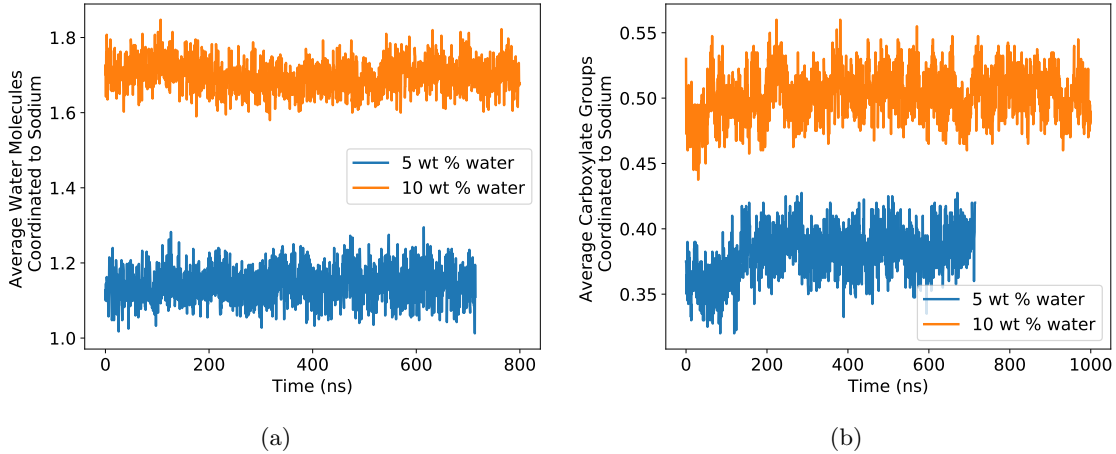
Mechanisms Governing Small Solute Transport

We observe trends in transport properties that are dependent on chemical environment within the nanopores as well as the chemical functionality of membrane constituents rather than just solute size.

- Polar solutes are slowed by interactions between monomer functional groups and ions.

6

- Solutes with hydrophobic character partition out of the pore and are slowed by densely packed organic monomer components.

- A thorough understanding of these interactions will help us to create monomer design principles.

- We will begin our analysis by considering the collective trends observed across all systems and then focus on subsets of similar molecules where some exceptions occur.

Like water and sodium above, the MSDs of the solutes studied in this work are significantly larger in the 10 wt % system, than those in the 5 wt % water system (Figure 4).

- The fastest moving solute in both cases, methanol, has an MSD about 175 times larger in the 10 wt % versus the 5 wt % system.

- Clearly the equilibrium water content of a given LLC system will determine its viability for real separations.

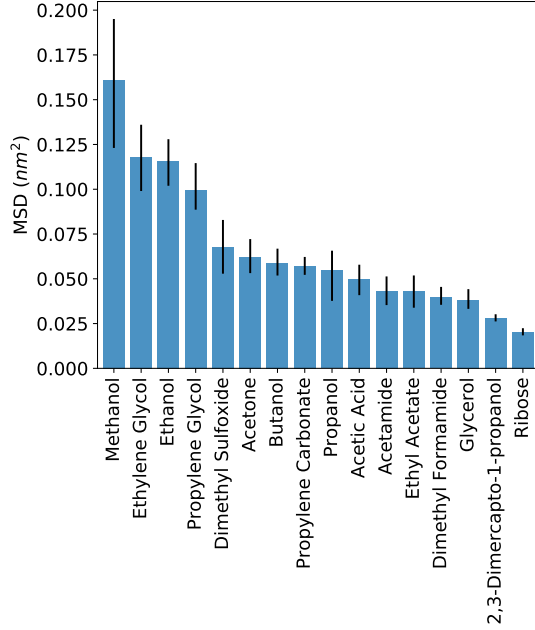The MSDs are not a monotonic function of solute size.

- We plotted the solute size against their MSDs in Figure 4c and 4d.

- There are numerous examples of solutes in our study that do not follow the behavior set forth by the Stokes-Einstein equation which implies that solute MSD should be inversely related to solute size.

- This behavior is not entirely surprising but worth emphasizing.

- It is expected that the Stokes-Einstein relationship, which assumes that the solute radius is much larger than the solvent, should break down once solute and solvent are of comparable size.

- Membranes, including that studied here, are often characterized with size-exclusion experiments which emphasizes selectivity based on the ability to enter a given pore.

- Once we reach the nm to sub-nm pore size regime, size-exclusion becomes of secondary importance since the primary purpose of these membranes is to separate molecules whose sizes are on the same order as water.

- In order to handle complex waste streams with molecules of similar size, it is important to take advantage of material properties other than pore size.

On the timescales simulated in our study, solutes exhibit subdiffusive behavior.

- Figure 5a plots the z-coordinate versus time of 3 representative ethanol centers of mass in the 10 wt % water system.

- There are clear periods of entrapment separated by relatively large hops.

- The MSD calculated based on all ethanol molecules is plotted in Figure 5b and is sublinear.

- The long periods of entrapment likely lead to this sublinear, and thus subdiffusive, behavior.

Solutes partition out of the pore into the head group region and beyond which may lead to radially dependent transport mechanisms.

- It is clear from Figure 5a that the longest periods of entrapment usually occur when solutes are far from the pore center.

- There is a high resistance to movement in the dense head group and tail regions.

- When hops occur, and where there is the most z-positional noise, solutes are generally close to the pore center.

- Solutes can move relatively freely when they enter the pore region which is primarily composed of water molecules and sodium ions.
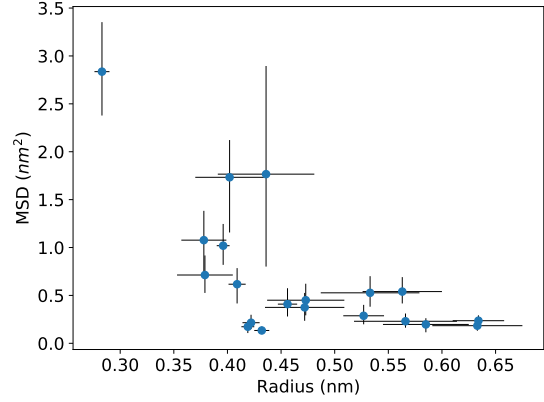
(a) 5 wt % water
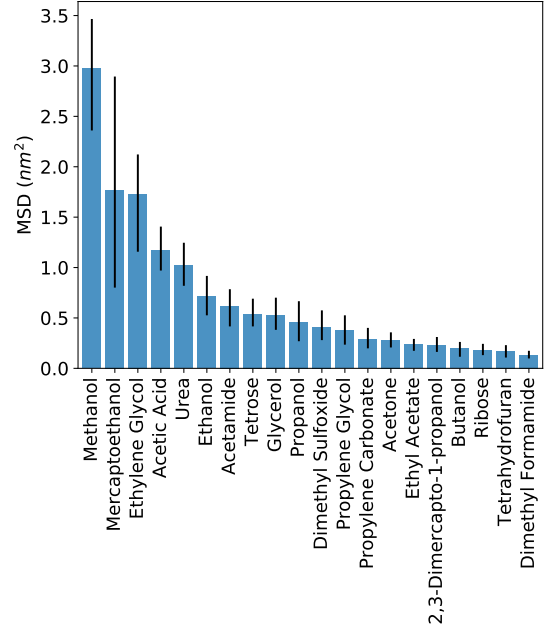
(b) 10 wt % water
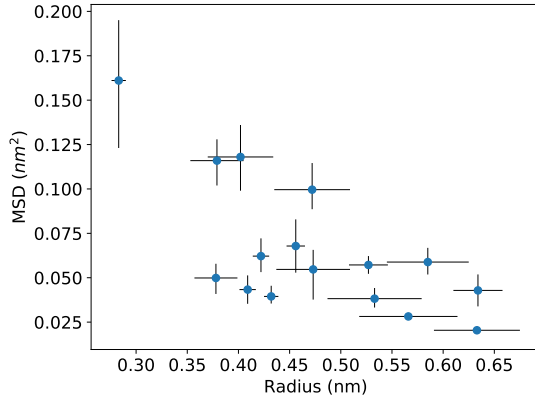
(c) 5 wt % water

(d) 10 wt % water

Figure 4: The MSDs of solutes in the 5 wt % water system (a) are significantly smaller than those of the solutes in the 10 wt % water system (b). The MSDs are not a monotonic function of molecular size (c and d).
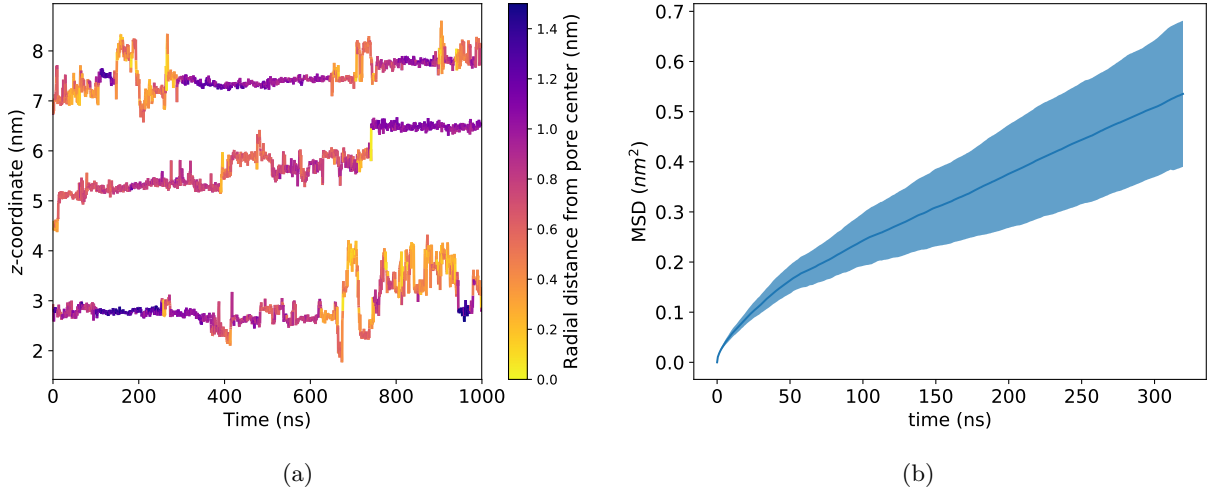
Figure 5: All solutes show subdiffusive transport behavior inside the membrane's nanopores, similar to that exhibited by ethanol. (a) The z-coordinate trace of 3 representative ethanol COMs shows clear periods of entrapment separated by hops. In general, the longest dwell times occur when solutes are situated far from the pore center and the hops occur when solutes are close to the pore center. (b) The time-averaged MSD of ethanol is not linear which suggests transport is governed by an anomalous subdiffusion process.

In addition to solute trapping in dense monomer regions, we observe a second trapping mechanism caused by preferential hydrogen bonding between hydrogen bond donor solutes and monomer carboxylate groups.

- Of the time spent donating hydrogen atom(s), x % of the hydrogen bonds occur between solutes and carboxylate groups as opposed to solutes with water.

- This shows a high preference for the carboxylate anions since there are 5 times more water molecules in the system.

- The carboxylate oxygen atoms have a slightly higher partial negative charge than water molecules.

- Additionally, on average, each sodium ion is coordinated to 1.7 water molecules. Roughly all of the water in the pore region is usually coordinated to a sodium ion which decreases their availability to solutes.

Finally, we see instances of solutes which become immobilized or slowed by association with sodium counterions.

- Much like water, the polarity of the solutes leaves partial negative charges which are stabilized through electrostatic interactions with sodium ions.

- There are many cases in which polar groups bind to sodium ions for at least a few time steps.

- There are some cases where solutes become immobilized for long periods of time while in close proximity to a sodium ion.

- In Figure 6, the oxygen atom of methanol stays within 2.5 Åof a sodium ion for the entire length of a trapping occurence.

The hopping and trapping mechanism exhibited by all solutes is characteristic of a continuous time random walk (CTRW) model.

- The length of entrapment follows a power law distribution (Figure 7a) and the distribution of hop lengths can be described with a Gaussian distribution (Figure 7b).
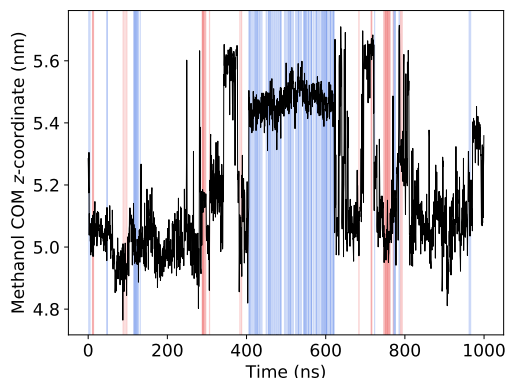
Figure 6: The oxygen atom of methanol stays bound to the same sodium ion for the majority of the trapping occurence between 400 and 600 ns. Regions highlighted red or blue indicate times when methanol's oxygen atom is within 2.5 Å of a sodium ion. The color of the shaded regions is switched every time the oxygen atom becomes associated to a different sodium ion.

- Power law distributed dwell times are responsible for the ageing phenomenon which causes the slope of the MSD curve to decrease with increasing measurement time because longer dwell times are sampled.

- Although these observed distributions strongly support a CTRW model, the time-averaged MSD of a pure CTRW should be linear which is not the case. [12, 13]

Transport may be better described by a subordinated fractional brownian motion (sFBM) model.

- Figure 7c shows the autocovariance function of ethanol step vectors.

- The negative autocovariance at low values of k indicates anti-correlation between hops.

- If solutes followed a pure CTRW mechanism, the autocovariance function would decay to zero immediately.

- Although the autocovariance function is relatively noise, due to the somewhat small number of hops observed over the course of each solute trajectory, there is the least uncertainty at k=1, the most insightful data point. This behavior is consistent across all solutes molecules.

- Therefore, we believe transport can be described as subordinated fractional Brownian motion where the leading process is a CTRW with hops whose direction is dictated by the parent process, FBM.

- Future publications will focus on modeling the solute's transport characteristics with an sFBM model

- We will draw on these observations only in a qualitative sense for the remainder of this work.

The transport behavior exhibited by solutes in the 5 wt % water systems is similar to those shown by those in the 10 wt % system however the timescales are much longer.

- We observe subdiffusive behavior with intermittent hopping between periods of entrapment.

- The frequency and length of hops are both diminished in the 5 wt % system.

- Since there are only 24 solute molecules in each system, in order to obtain better time-averaged descriptions of solute transport mechanisms, we will focus the rest of our analysis on transport in the 10 wt % water systems.
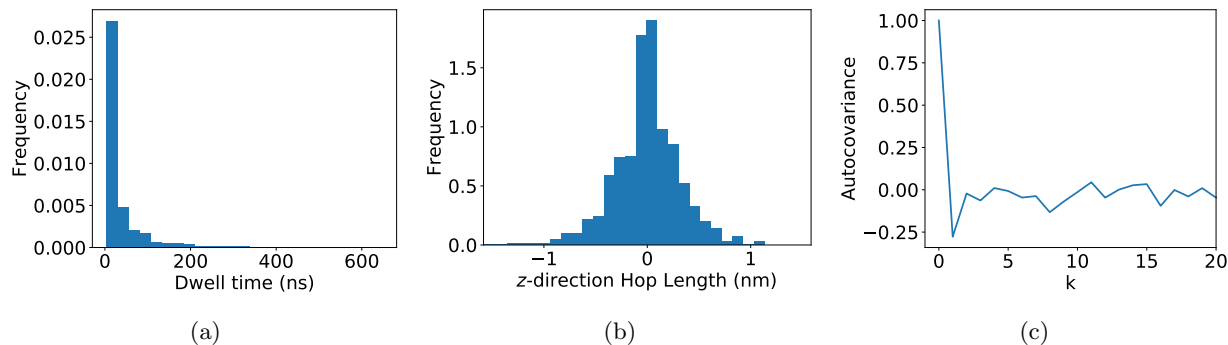
Figure 7: (a) The distribution of dwell times resembles a power law distribution. (b) The distribution of hop lengths appears Gaussian. (c) Hops are anti-correlated to their previous hop as indicated by the negative value of the autocovariance function at $k = 1$.

Transport of Simple Alcohols

The MSD of methanol, ethanol, propanol and butanol descends in order of their molecular weight, however, methanol travels faster than expected.

- The MSD of ethanol, propanol and butanol descend approximately linearly as expected from the Stokes-Einstein relationship

- However, methanol travels considerably faster than suggested by the relationship. (See Figure 8a

Methanol moves fast, not only because it is the smallest solute studied in this work, but because it has the highest radial density near the pore center where the largest hops occur.

- The radial density as a function of distance from the pore center for each alcohol is plotted in Figure 8b.

- On average, the density of methanol in the pore center is only slightly less than the density near the head groups.

- All other alcohol molecules are most concentrated in the head group region.

All simple alcohols participate in a similar number of hydrogen bonding interactions with the monomer head groups, but with varying preference towards hydrogen bonds with the monomer carboxylate oxygen atoms (See Figure 8c) caused by increasing hydrophobic character.

- If all 5 hydrogen bonding acceptor sites on the monomer head groups were equal, we would expect the ratio of the number of hydrogen bonds between solutes and the two carboxylate oxygen atoms to the number of hydrogen bonds between solutes and the three ether groups to be 2/3.

- There is a clear preference towards hydrogen bonding with the carboxylate oxygen atoms for all simple alcohols.

- This is largely due to the more highly crowded environment surrounding the ether oxygen atoms combined with their lower partial charges.

- Butanol shows the largest preference towards hydrogen bonds with carboxylate head groups.

- The radial distribution function of atoms located at opposite ends of butanol shows that, on average, oxygen atoms are situated 0.25 nm closer to the pore centers than the distal carbon atoms.

- This suggests that alcohols tend to orient themselves like the liquid crystal monomers, with hydrophilic components point towards the pore centers.

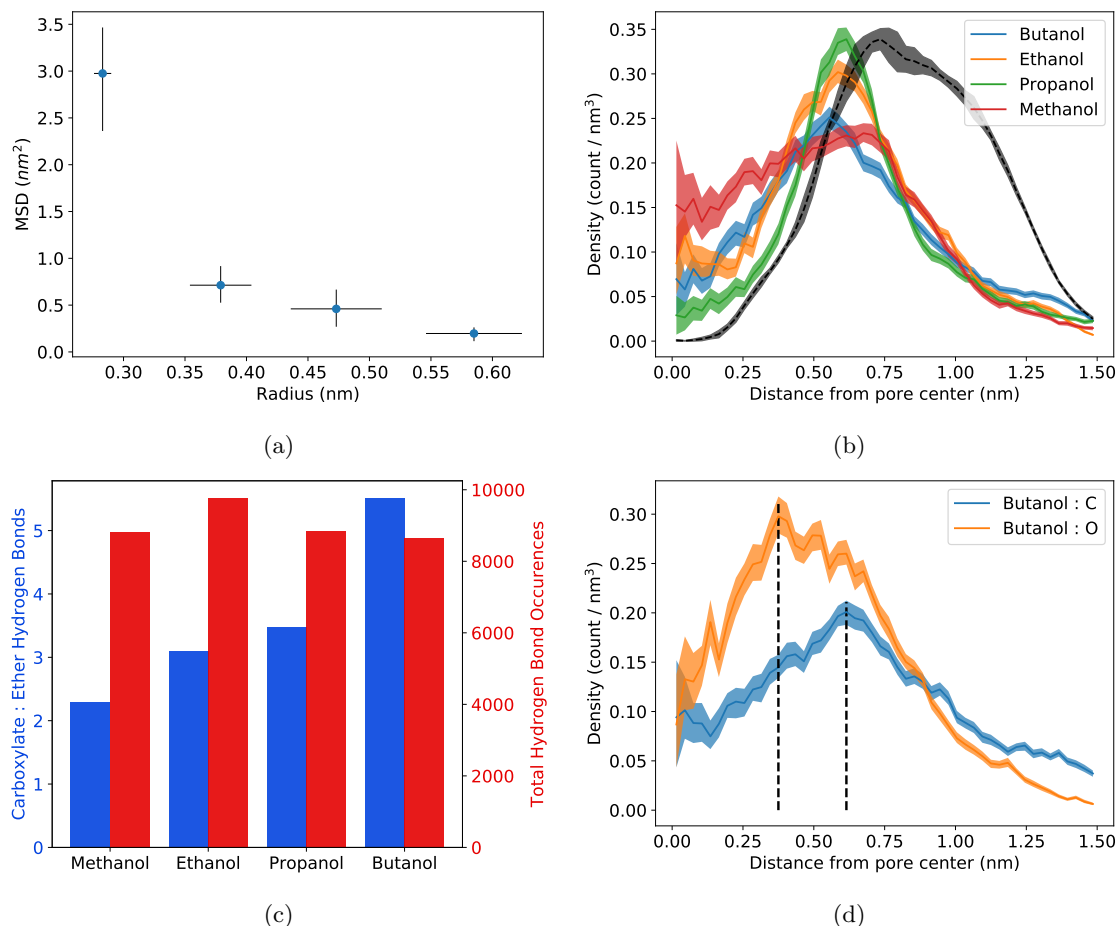- When solutes are buried in the pore walls, their MSDs are shorter.

11

Figure 8: (a) The MSD of the simple alcohols decrease as a function of the solute size, however methanol's MSD is considerably higher than expected based on the Stokes-Einstein equation. (b) The radial distribution functions of each simple alcohol shows a maximum close to the highest density of monomer head groups (dashed line, normalized for easier visual comparison). Methanol spends the largest proportion of time, relative to the other alcohols, near the pore center, which may help explain its fast dynamics. (c) Despite relatively little difference in the total number of hydrogen bond occurences, a given alcohol's preference towards hydrogen bonds with the carboxylate groups increases with molecule size. (d) The average location of butanol's oxygen atom is significantly closer to the pore center than its most distal carbon atom, suggesting that the molecule is oriented with hydrophobic tails pointing away from the pore center.

Transport of Diols, Triols and Sugars

The order of the MSDs of solutes in this grouping are roughly consistent with their size, however propylene glycol moves exceptionally slow.

- Ethylene glycol has the highest MSD followed by tetrose and glycerol, whose MSDs are similar, propylene glycol, the second smallest solute of this set, and finally ribose.

Transport is both facilitated and hindered by additional solute hydroxyl groups due to their influence on radial density and hydrogen bond frequency.

- Extra hydroxyl groups cause solutes to favor the water-rich pore region. where there is the least hindrance to movement (See Figure 9a).

- Tetrose, ribose and glycerol are densest close to the pore center. This is likely a result of their hydrophilicity and large size which prevents them from partitioning into the head group region.

- However, these extra hydroxyl groups facilitate a larger number of hydrogen bond interactions that work to hold solutes in place (See Figure 9).

- It has been observed that hydrogen bonding in a system will generally reduce diffusivity [14]

The number of hydrogen bonding interactions between solutes and head groups increases with the number of solute hydroxyl groups.

- These solutes frequently undergo simultaneous hydrogen bond interactions as shown in Figure 9.

- For example, both hydroxyl groups of ethylene glycol can undergo hydrogen bonds with different hydrogen bond acceptors at the same time.

- In some cases, all 4 hydroxyl groups of ribose are hydrogen bonded to monomer head groups simultaneously.

- Hydrogen bonds act as a kind of molecular glue which holds solutes in place, especially when there are many, however proximity to the pore center partially compensates for this effect in the cases of glycerol and tetrose.

Of the two diols, ethylene glycol moves significantly faster than propylene glycol due to propylene glycol's affinity for the monomer head groups.

- Combined with an increase in size, the addition of a single methyl group to ethylene glycol increases propylene glycol's hydrophobic character and causes it to favor positions near monomer head groups.

- Both diols have comparable densities close to the pore center, however propylene glycol's density has a large peak near the monomer head groups relative to ethylene glycol.

- Propylene glycol can form more highly stablized hydrogen bonds with carboxylate groups, explaining the higher incidence of hydrogen bonds shown in Figure 9.

- These observations are further reflected in its dwell and hop length distributions (See Figure 9c).

- Propylene glycol exhibits longer dwell times and a narrower distribution of hop lengths than ethylene glycol.

- Somewhat counterintuitively, there is a relatively high density of ethylene glycol molecules beyond the head group region probably due to its relatively small size. This likely contributes to the somewhat large error bars on its MSD in Figure 4.

- This implies that hops performed by ethylene glycol must be considerably larger than those by propylene glycol in order to result in consistently larger MSD values.
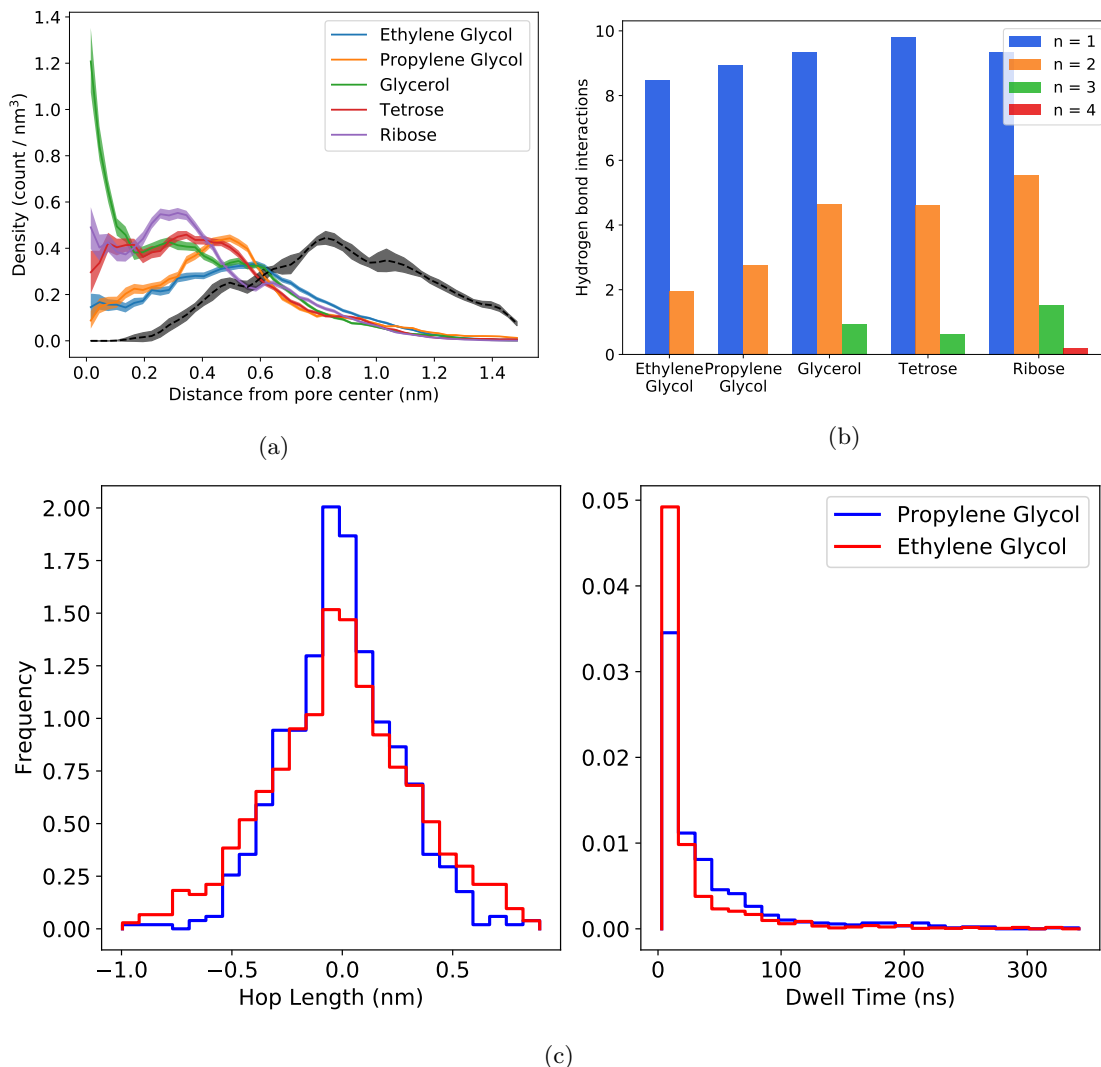
(a)

(b)

(c)

Figure 9: The number of hydrogen bond interactions between solutes and monomers increases as solutes gain additional hydroxyl groups. Multiple hydroxyl groups within a solute often hydrogen bond in different locations simultaneously. Occasionally, all four hydroxyl groups of Ribose (n = 4) are involved in a hydrogen bond interaction at the same time.

Transport of Ketones and Amides

The 4 ketone-like molecules tested show a surprising range of transport behaviors.

- Urea, acetic acid, acetamide and acetone are all characterized by a carbonyl group with two attached heavy atoms.

- All are similar in size and are planar molecules due to the sp2 hybridization of their carbonyl group.

- The fastest solute of this grouping, acetic acid (comparable to urea), is about 3 times faster than the slowest, acetone, but only about 10 % smaller.

The MSD of the solutes descend in order of their density close to the pore center.

- As shown in the radial density functions (Figure 10a), Acetic acid has a fairly uniform and high density within the pore region.

14

- Acetone spends relatively little time near the pore center with its peak density nearest the peak head group density.

The amides, urea and acetamide, hydrogen bond with head groups relatively infrequently, but regularly coordinate with sodium ions (See Figure 10).

- In an average frame, acetic acid participates in more than 12 hydrogen bonds with monomer head groups while urea and acetamide participate in less than 2.

- Urea and Acetamide both have hydrogen bond donating nitrogen atoms, however nitrogen is a weaker hydrogen bond donor than oxygen due to its lower electronegativity.

- Given their lower propensity to hydrogen bond one might expect amides to partition out of the pore and/or to move through the pore quickly, perhaps faster than methanol.

- The peaks in their radial density are still situated between the pore center and the head groups, but closer to the pore center than other solutes that hydrogen bond with carboxylate groups (see Figure 8b, for example).

- Both solutes spend about half of their time with their carbonyl oxygen atom coordinated to a sodium ion which restrains the solutes to within the pore region

- Interestingly, the nitrogen atoms do not coordinate with any sodium ions despite a similar negative partial charge. The hydrogen atoms may shield this interaction.

Acetone has the lowest MSD of this set because it is primarily trapped near and behind the head groups.

- On average, acetone coordinates with sodium with the same frequency as acetic acid

- However, acetic acid spends more time in the pore center and therefore encounters more sodium ions.

- When an acetone molecule coordinates with a sodium ion, its polarity is largely neutralized and it retreats towards the head group region where it can easily get trapped.

- Acetic acid and the amides and acetic acid have alternate hydrophlic groups when bound to sodium ions which increases their stability in the pore.

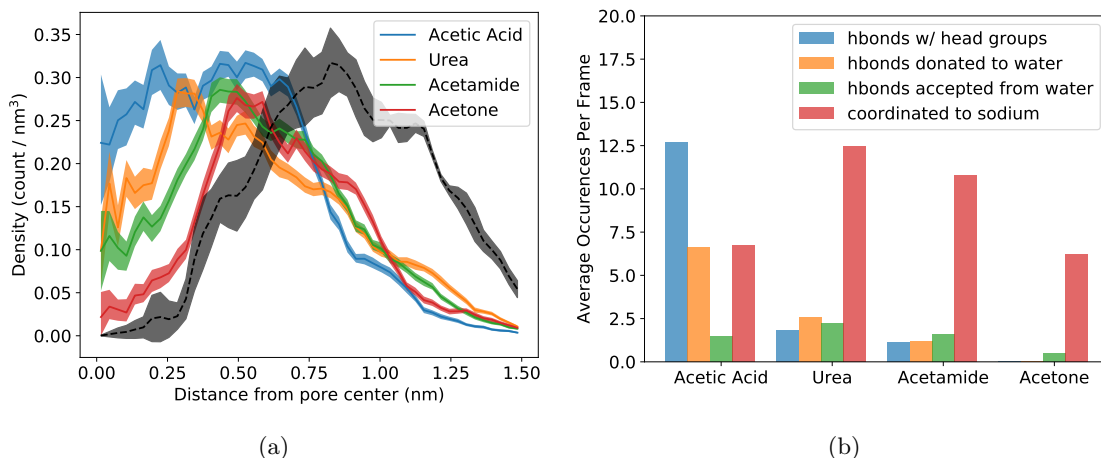(a)   (b)

Figure 10: (a) The radial density near the pore center (r = 0) decreases with decreasing solute MSD. (b) The amides hydrogen bond with water far less than acetic acid, however they tend to coordinate with sodium ions more frequently.
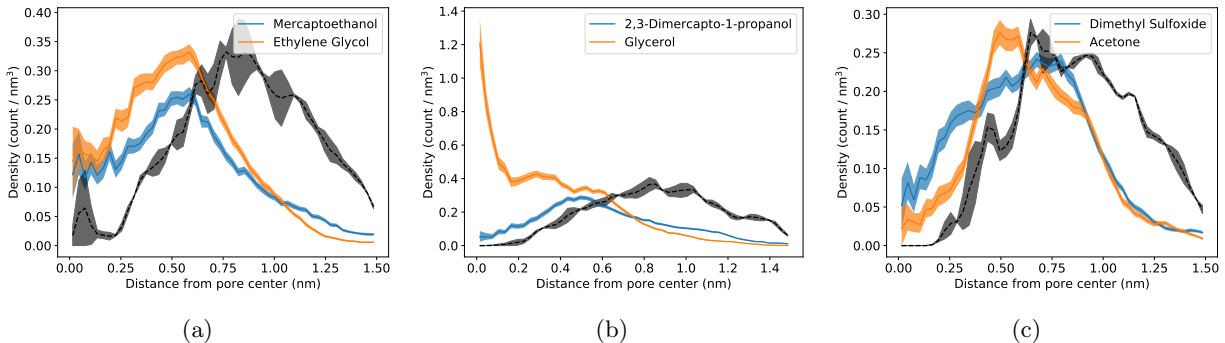
15

Figure 11

Transport of Thiols

We also studied the transport properties of sulfur analogs of glycerol, ethylene glycol and acetone.

- We replaced all but one oxygen atom of ethylene glycol and glycerol with sulfur atoms to create Dimercaptoethanol and 2,3-Dimercapto-1-propanol.

- We replaced the carbonyl carbon of acetone with sulfur in order to create DMSO.

- Sulfur is unable to hydrogen bond, however it is soluble in water

Mercaptoethanol has a similar average MSD and RDF to ethylene glycol.

- There is a much larger uncertainty associated with mercaptoethanol's MSD.

- It spends more time in the tail region than ethylene glycol, where transport is inherently slower, and may contribute to some slower MSDs.

- Conversely, Mercaptoethanol also exhibits some of the highest single solute MSDs (See Figure 12a)

- It hydrogen bonds with head groups 6 times less frequently than ethylene glycol.

- This may lead to larger hops in the pore region.

- Some of this can be accounted for by the higher density of mercaptoethanol molecules in the head group / tail region. There are nearly 40 % more mercaptoethanol molecules than ethylene glycol molecules beyond 0.8 nm from the pore center.

2,3-Dimercapto-1-propanol exhibits slower transport than glycerol because it spends more time near monomer head groups.

- Glycerol frequently hydrogen bonds with more than one head group at a time (See Figure 9).

- It can also hydrogen bond with water molecules which increases its stability in the pore region.

- 2-3-Dimercapto-1-propanol preferentially hydrogen bonds with head groups so it gravitates towards the head group region.

DMSO has a comparable if not large MSD than acetone even though it is a slightly larger molecule.

- The radial density of DMSO is higher than acetone close to the pore center.

- The pyramidal structure of DMSO may force it to spend more time closer to the pore center.

16
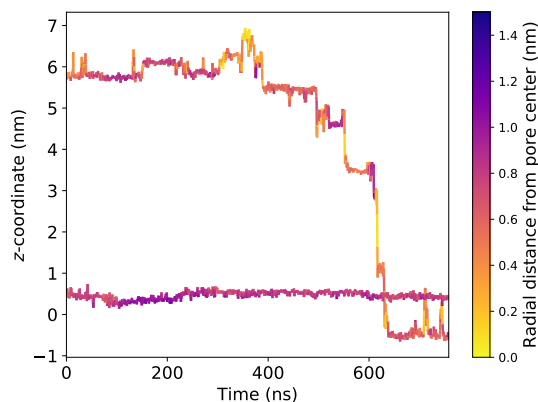
(a)

Figure 12: Mercaptoethanol exhibits transport behavior ranging from frequent hopping to lengthy trapping. Large hops generally occur near the pore center while long entrapments occur while tangled among the monomer tails.

Hydrogen bond acceptors

The slowest set of molecules we studied can accept hydrogen bonds, but cannot donate them.

- Among this set are the two slowest solutes in our study: Tetrahydrofuran and Dimethyl Formamide.

- The MSDs of ethyl acetate, propylene carbonate and acetone are only marginally larger.

The radial density of solutes near the pore center in this set is surprisingly high as shown in Figure 13a.

- Propylene carbonate and ethyl acetate are among the largest solutes in this study. Their size prevents them from easily entering the tail region and generally gives faster transport properties since they spend more time in the pore region.

- However, this is not a hard rule. When a solute does overcome the barrier of entry beyond the head group region, it can become trapped. All solutes in this set show a peak geq 1 nm from the pore center which is likely caused by solutes that get trapped in the tail region for a significant amount of time.

- The peak density of THF is considerably offset from the pore center.

- Observations of single THF trajectories have revealed that it does not make large hops while in the pore center.

- THF becomes nearly immobilized while associated with sodium ions (See Figure 14).

- DMF experiences a similar effect, but to a lesser extent. Its density is higher than THF near the head groups. The planar shape of DMF causes it to become stuck between head groups. Excursions into the pore region do not necessarily result in large hops.

Carbonyl groups continue to show high degrees of association with sodium ions.

- The number of sodium ions coordinated to the carbonyl group of propylene carbonate, dimethyl formamide, ethyl acetate are consistent with that shown by acetone, all between 6 and 7 per frame (See figure 13b)

- The carbonyl group of the amides studied in the previous section associate with sodium nearly twice as frequently as compounds that don't contain nitrogen (see figure 10b).

- In all cases, other polar groups on carbonyl-containing compounds associate with sodium in negligible amounts.

17

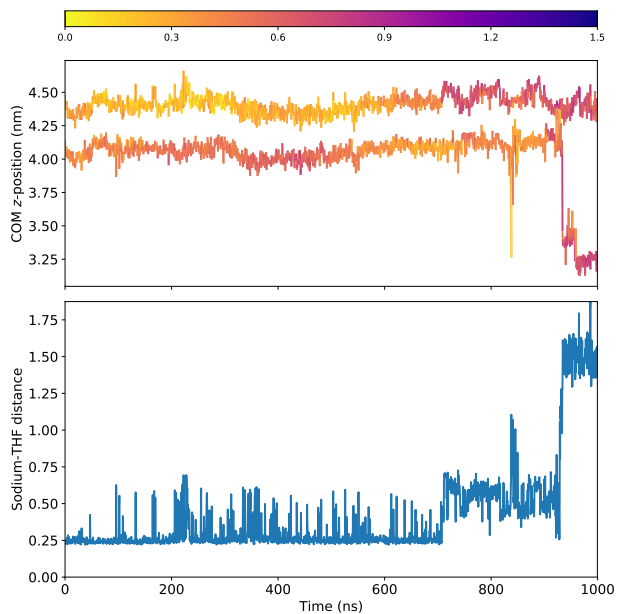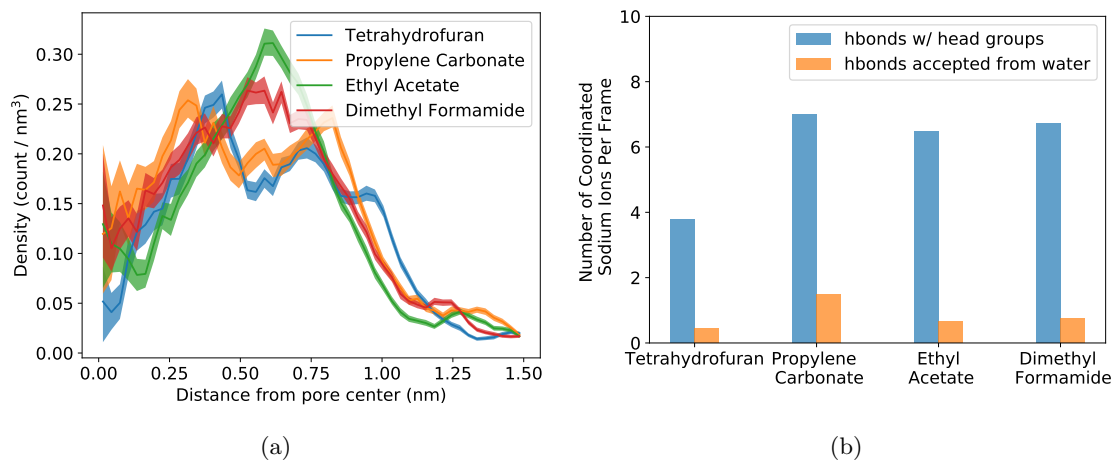(a)   (b)

Figure 14: Coordination of THF with sodium ions may help stabilize it inside the pore region. For the first 700 ns of the trajectories shown, the center of mass of THF (top line in top figure) and a sodium ion (bottom line in top figure) move in tandem. The distance between the oxygen atom of THF and the sodium ion has only occasional fluctuations away from a relatively stable separation of ca. 0.25 nm. After 700 ns, THF separates from the sodium ion and moves closer to the head group region.

3.1 Design Principles

Water content affects pore size and strongly influence the MSD of both solutes and water. Experiments to understand how controllable this parameter is could be useful.

Two routes one might want to go down:

1. Only allow water to pass

2. Selective separation of a dissolved species.

Monomers that cannot hydrogen bond.
Separate polar molecules by creating monomers with head group components designed to hydrogen bond.

- Hbond donors

- More incentive to dwell on walls.

Ions with less water coordination (or more water) so that solutes can hbond with water and perhaps be more inclined to stay in the pore region.

4 Conclusion

We have examined the transport characteristics of a series of small polar molecules in our model of the H_{II} phase formed by Na-GA3C11.

We calculated the macroscopic diffusion coefficients of each solute as approximated by a CTRW model and validated our estimates using experimental DOSY NMR measurements.

We have studied the influence of water content on the diffusion coefficients.

We showed that hydrogen bonding between solutes and Na-GA3C11 monomers plays a major role in mechanism by which molecules traverse the nanopores.

We can use this intuition in order to modify our monomers for a specific separation.

- Increase number of h-bond sites to increase selectivity towards water over polar molecules

Supporting Information

Detailed explanations and expansions upon the results and procedures mentioned in the main text are described in the Supporting Information. This information is available free of charge via the Internet at http://pubs.acs.org.

Acknowledgements

References

[1] R. C. Smith, W. M. Fischer, and D. L. Gin, "Ordered Poly(p-phenylenevinylene) Matrix Nanocomposites via Lyotropic Liquid-Crystalline Monomers," *J. Am. Chem. Soc.*, vol. 119, no. 17, pp. 4092–4093, 1997.

[2] M. Zhou, P. R. Nemade, X. Lu, X. Zeng, E. S. Hatakeyama, R. D. Noble, and D. L. Gin, "New Type of Membrane Material for Water Desalination Based on a Cross-Linked Bicontinuous Cubic Lyotropic Liquid Crystal Assembly," *J. Am. Chem. Soc.*, vol. 129, pp. 9574–9575, Aug. 2007.

[3] R. Resel, U. Theissl, C. Gadermaier, E. Zojer, M. Kriechbaum, H. Amenitsch, D. Gin, R. Smith, and G. Leising, "The H2-Phase of the Lyotropic Liquid Crystal Sodium 3,4,5-Tris(omega-Acryloyloxyundecyloxy)benzoate," *Liq. Cryst.*, vol. 27, pp. 407–411, Mar. 2000.

[4] B. J. Coscia, J. Yelk, M. A. Glaser, D. L. Gin, X. Feng, and M. R. Shirts, "Understanding the Nanoscale Structure of Inverted Hexagonal Phase Lyotropic Liquid Crystal Polymer Membranes," *J. Phys. Chem. B*, vol. 123, pp. 289–309, Jan. 2019.

[5] Y. Meroz and I. M. Sokolov, "A Toolbox for Determining Subdiffusive Mechanisms," *Physics Reports*, vol. 573, pp. 1–29, Apr. 2015.

[6] R. Metzler, J.-H. Jeon, A. G. Cherstvy, and E. Barkai, "Anomalous Diffusion Models and Their Properties: Non-Stationarity, Non-Ergodicity, and Ageing at the Centenary of Single Particle Tracking," *Phys. Chem. Chem. Phys.*, vol. 16, pp. 24128–24164, Oct. 2014.

[7] C. Truong, L. Oudre, and N. Vayatis, "Ruptures: Change Point Detection in Python," Jan. 2018.

[8] A. Luzar and D. Chandler, "Effect of Environment on Hydrogen Bond Dynamics in Liquid Water," *Phys. Rev. Lett.*, vol. 76, pp. 928–931, Feb. 1996.

[9] D. Prada-Gracia, R. Shevchuk, and F. Rao, "The quest for self-consistency in hydrogen bond definitions," *J. Chem. Phys.*, vol. 139, p. 084501, Aug. 2013.

[10] C. N. Rowley and B. Roux, "The Solvation Structure of Na+ and K+ in Liquid Water Determined from High Level ab Initio Molecular Dynamics Simulations," *J. Chem. Theory Comput.*, vol. 8, pp. 3526–3535, Oct. 2012.

[11] J. Ma, K. Li, Z. Li, Y. Qiu, W. Si, Y. Ge, J. Sha, L. Liu, X. Xie, H. Yi, Z. Ni, D. Li, and Y. Chen, "Drastically Reduced Ion Mobility in a Nanopore Due to Enhanced Pairing and Collisions between Dehydrated Ions," *J. Am. Chem. Soc.*, Feb. 2019.

[12] T. Neusius, I. Daidone, I. M. Sokolov, and J. C. Smith, "Subdiffusion in Peptides Originates from the Fractal-Like Structure of Configuration Space," *Phys. Rev. Lett.*, vol. 100, p. 188103, May 2008.

[13] Y. Meroz, I. M. Sokolov, and J. Klafter, "Subdiffusion of mixed origins: When ergodicity and nonergodicity coexist," *Phys. Rev. E*, vol. 81, p. 010101, Jan. 2010.

[14] G. Srinivas, S. Bhattacharyya, and B. Bagchi, "Computer simulation and mode coupling theory study of the effects of specific solutesolvent interactions on diffusion: Crossover from a sub-slip to a super-stick limit of diffusion," *J. Chem. Phys.*, vol. 110, pp. 4477–4482, Feb. 1999.

TOC Graphic